ICAST2015: 26th International Conference on Adaptive Structures and Technologies
October 14-16th, 2015, Kobe, Japan

ICAST2015 041

On an efficient implementation of non-linear structural optimization for the morphing leading edge of an active blown high lift system.

Michael Rose[1*], Anton Rudenko[1], and Hans Peter Monner[1]

[1] Institute of Composite Structures and Adaptive Systems,
German Aerospace Center (DLR), Braunschweig, Germany.

Abstract

The permanently increasing demands on performance and noise reduction in today's aircraft high lift systems enforces the study of adaptive technologies to overcome the restrictions of state of the art fully passive technologies. As an alternative to conventional slats and flaps, an active blown Coandă-flap based high lift system is investigated within the German national Collaborative Research Centre 880 to improve on the mentioned limitations. One key feature is provided by an adaptive gapless droop nose with an exceedingly high grade of leading edge morphing. The construction of this component is based on a structural optimization framework, developed at DLR. The framework consists of two hierarchical design steps, an optimization of the skin layout with discrete joints to the inner actuation mechanism and the topology optimization of the latter.

In this paper, the methodology of the second step and its application to the droop nose is discussed. For efficiency reasons, the design of the inner mechanism is completely implemented in the matrix software environment MATLAB. A key component is given by a Finite Element based non-linear solver for the static calculation of the stiffness distribution on a regular grid. As part of the inner loop of this design process, this solver must be implemented as efficient as possible. Due to the lack of sensitivity information in commercial Finite Element programs, the direct implementation of the elasticity equations is further enforced. A main focus of this article concentrates on the underlying assembly approach for the needed system matrices. Finally the application of the tool chain to the droop nose compliant mechanism is presented.

1. INTRODUCTION

The flow control system shown in Figure 1 takes advantage from the Coandă-effect to enhance the flight characteristics of an airplane wing in different flight conditions. It is one of the considered approaches within the framework of the Collaborative Research Center 880 (SFB880). An important component consists of a device capable to adapt its shape according to aerodynamic requirements without any structural gaps or steps. There have been many aerospace research activities in the field of morphing aircraft structures, starting with the flight of the Wright Flayer I. Good reviews are given in [1, 2].

This paper discusses the shape and camber morphing of the airfoil. In constract, the established technique of wing camber changing to enhance the low speed capabilities in commercial aircrafts results in

* info@icast2015.com

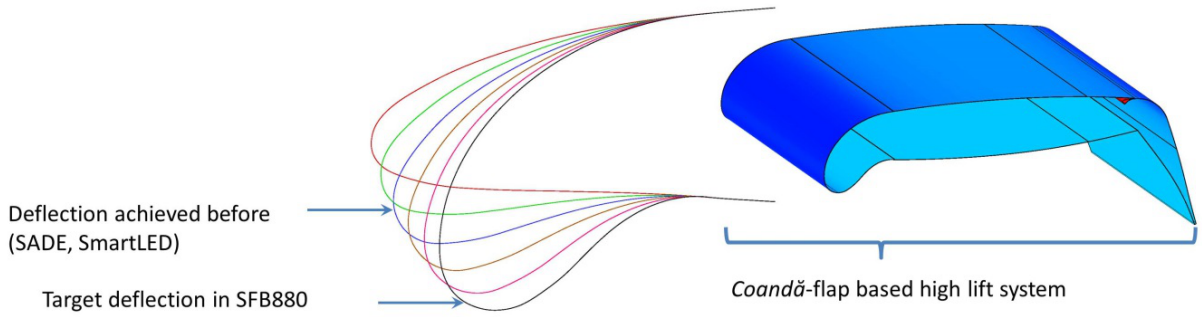

Figure 1. Coandă-flap based high lift system and the deflection of the adaptive droop nose

complex mechanical systems without the ability to provide a stepless aerodynamic shape. The substitution of such systems by less complex adaptive structures without any gaps and steps is very promising to achieve improvements in efficiency. Though such kind of leading edge devices have been successfully presented in [3, 4] as a result of the European project "Smart High Lift Devices for Next Generation Wings" (SADE), the achievable deflection is limited by the considered design. Therefore the considerably higher level of non-linear morphing, which is needed by the Coandă-flap based high lift system with circulation control as described in [5], presents an additional challenge in SFB880. From the structural point of view, this challenge can be separated in some research domains:

- Development of a skin that is flexible enough to sustain the desired shape change and is also stiff enough to carry the aerodynamic loads.
- Design and creation of a morphing mechanism for transferring actuator forces to the skin and aerodynamic loads to the wing structure.
- Definition of an appropriate interface between the skin and the mechanism to provide the desired deformation accordingly to the aerodynamically reasonable target shape.

The skin concept is developed at the Institute of Aircraft Design and Lightweight Structures (Technical University of Brunswick) within the framework of SFB880 and the design relies on input provided by the present work, consisting of the stiffness distribution of the skin. To reach the morphing demand, highly anisotropic materials in combination with enhanced stiffness tailoring is used to overcome the restrictions of conventional composite skins. The morphing mechanism is investigated at the Institute of Composite Structures and Adaptive Systems (German Aerospace Center).

The goal of the topology optimization is to exchange conventional mechanisms like the ones shown in Figure 2 with inner compliant mechanisms to reduce the weight and the need for inner joints simultaneously. The discussion of the methodology and the current status is a central point in this paper.

2. A PROCESS CHAIN FOR STIFFNESS AND TOPOLOGY OPTIMIZATION

Optimization of the skin stiffness distribution has doubtless to be coupled to the optimization of the inner kinematics of the droop nose device, because these are parts of one elastic system and have decisive influence on the shape quality. On the other hand, these two parts have some different requirements

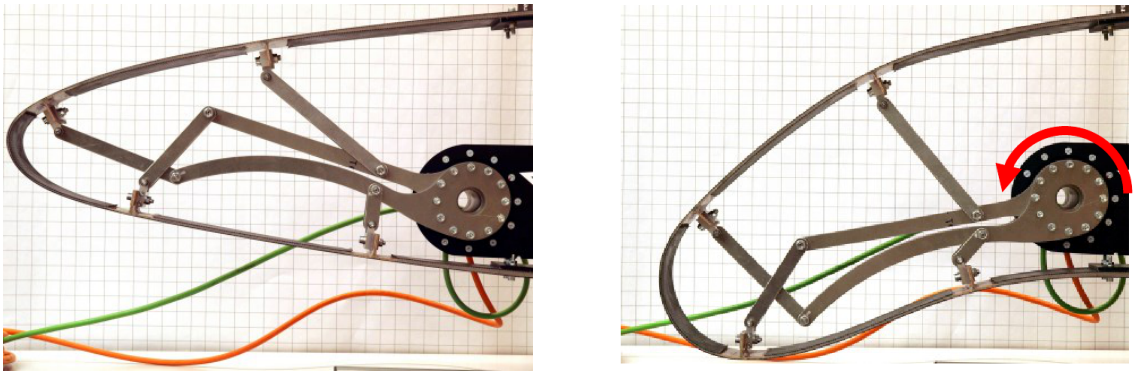

Figure 2. Demonstrator of an adaptive droop nose in normal flight (left) and high lift (right) configuration

towards boundary conditions, applicable optimization methods and parameters: the most important demand on the skin is to provide a reasonable curvature according to the given aerodynamic target shape, but the inward actuating mechanism is more restricted by material loads and weight considerations.

In keeping with this, a two-stage optimization framework shown in Figure 3 (left) was developed to combine these requirements. The first part of the framework handles the stiffness tailoring of the skin and interface elements between the skin and kinematics, described in section 3.

To perform further optimization of the inner kinematics, the skin stiffness data has to be stored and provided to the next optimization step. For this reason, the stiffness matrix of the skin and the force vectors of the actuation nodes have to be stored in so-called "superelements" — substructures, that means in matrices which describe the elastic behavior of the structure in the working point. The substructuring procedure can handle large deflections and rotations of the given problem as long as the local strains remain low (about one percent in the present work). Further description of the substructuring approach for non-linear solutions can be found in [6, 7]. With this structural information, the next optimization step, described in section 4 can be initiated.

3. SKIN STIFFNESS TAILORING

The skin optimization tool is based on a finite element implementation of the droop nose skin with spanwise oriented stringers acting as force application points for the inward kinematic. The skin is modelled with shell elements, allowing the application of composite and hybrid materials. The design parameters of the skin stiffness optimization routine are:

- the stiffness distribution along the airfoil circumference (variable GFRP-layup)
- the locations of the kinematic - skin interfaces
- the direction and amount of the actuation forces at these locations

The objective function is given by the distance between the calculated skin deformation and the target shape provided by a foregone aerodynamic optimization. The optimization constraint is the maximal

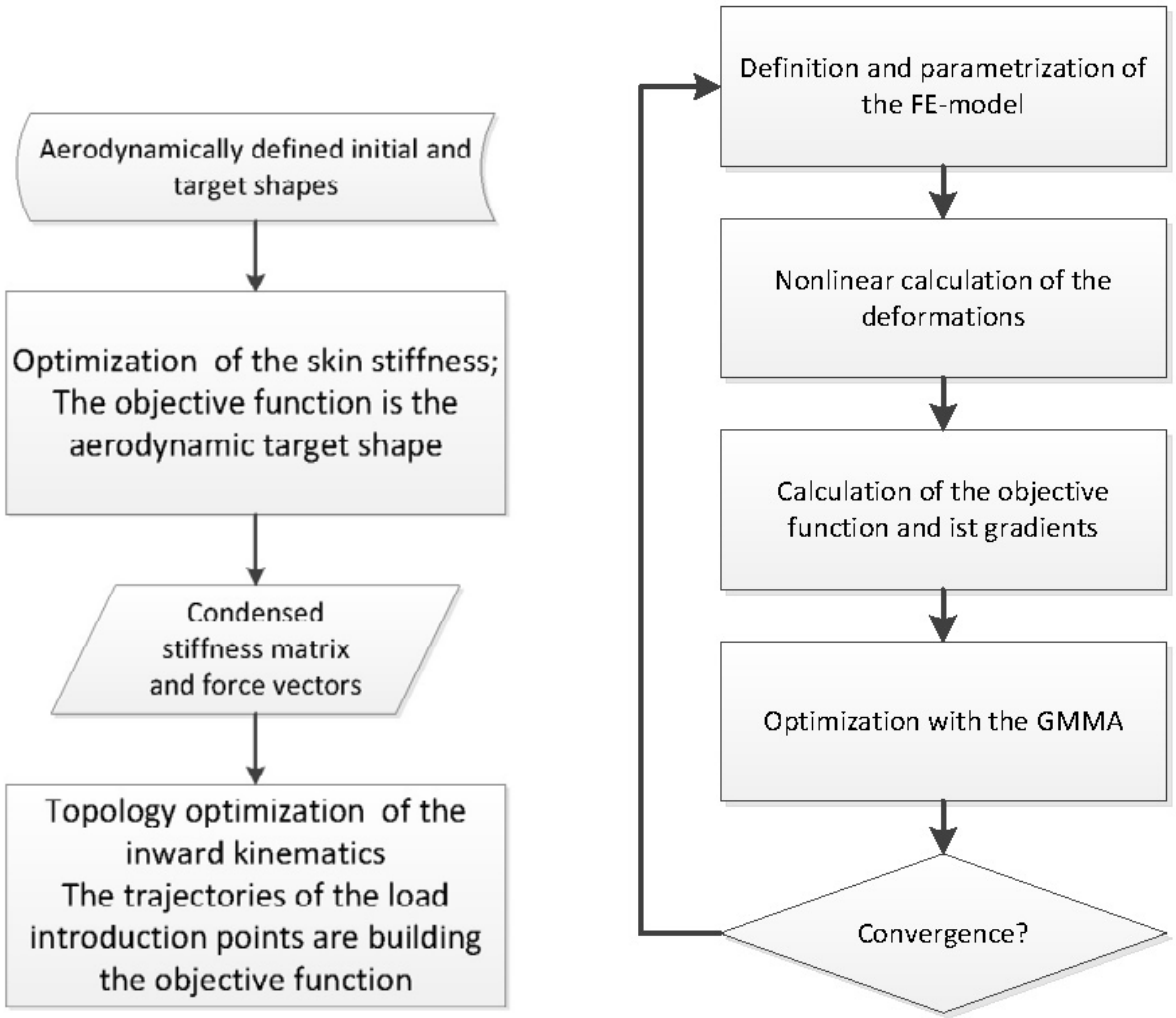

Figure 3. The subdivision of the optimization process chain (left) and the workflow of the topology optimization (right)

elastic strain of the material:

$$\frac{\epsilon_\ell}{\epsilon_{\max}} - 1 \leq 0 \tag{1}$$

Strains and deformations of the skin are calculated with a non-linear ANSYS solver and the optimization is performed with MATLAB-integrated simplex algorithm. An example result of the optimization is presented in Figure 4 (left).

Another important question is the kind and the geometry of the force introduction elements between the skin and the kinematics. In previous projects omega-stringers were chosen mainly because of the robustness and structural strength of this concept. On the other hand, an omega-stringer on a flexible morphing skin results in strong discontinuity of the skin stiffness. A resulting effect on the shape curvature of the morphed airfoil is disadvantageous for the aerodynamic flow and therefore has to be

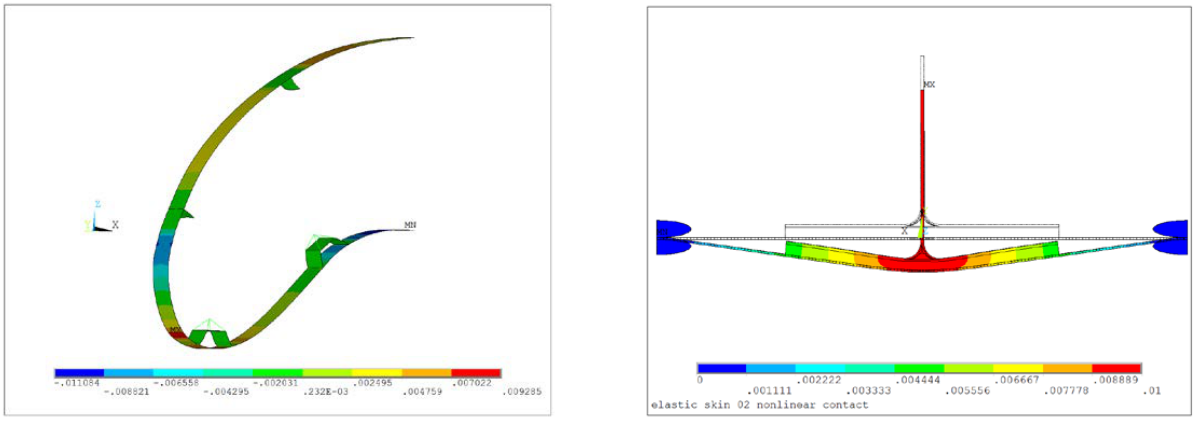

Figure 4. An example of a deformed skin with Omega- and T- stringers, acting as force introduction elements (left) and three-point bending model of a T-stringer on the flexible hybrid elastomer-GFRP skin (right)

minimized.

Based on these considerations a sensitivity analyses was performed to determine an optimal number and type of the force introduction elements to be applied. Additionally to Omega-stringers, T-, L- and I-stringer types were implemented in the optimization loop to investigate the curvature effects.

Some selected results of this analysis are shown in Figure 5, where two optimized droop nose skins with different force introduction concepts are compared regarding the deviation from the target shape and its curvature. It is identifiable that, although the deviations from the target shape are quite small for both concepts, the shapes of the curvature graphs are rather different: The curvature plot of the concept in the Figure 5 (left) shows a generally less continuous behavior with a zero passage (marked with a red circle) by 45 percent of the skin perimeter. Such behavior (especially the zero crossing) of the curvature is well known for disturbance of the aerodynamic flow by disadvantageous pressure gradients. Whereas concept presented in the Figure 5 (right) provides clearly better curvature and can be identified as more appropriate for the morphing skin application.

Having better capabilities as force introduction elements regarding the curvature, T-stringers are less reliable than Omega-stringers regarding the structural strength and stability. To prove the concept, the T-stringer was implemented in a parametric high fidelity finite element model with layered solid elements, shown in Figure 4 (right).

4. TOPOLOGY OPTIMIZATION OF THE INWARD KINEMATICS

For the topology optimization of the complained kinematic mechanism, the Solid Isotropic Material with Penalization (SIMP) was applied. This method is described by Sigmund and Bendsøe in [8, 9] for linear finite element calculations and was extended for non-linear systems. A further step to non-linear analysis like it was applied in this work was presented by Saxena and Ananthasuresh in [10]. The workflow of the optimization routine is described in Figure 3 (right). In order to have the necessary full access to the stiffness matrix and element densities of the compliant kinematic, a proprietary non-linear finite element grid solver was implemented in C/Matlab. The solver allows calculating of grid

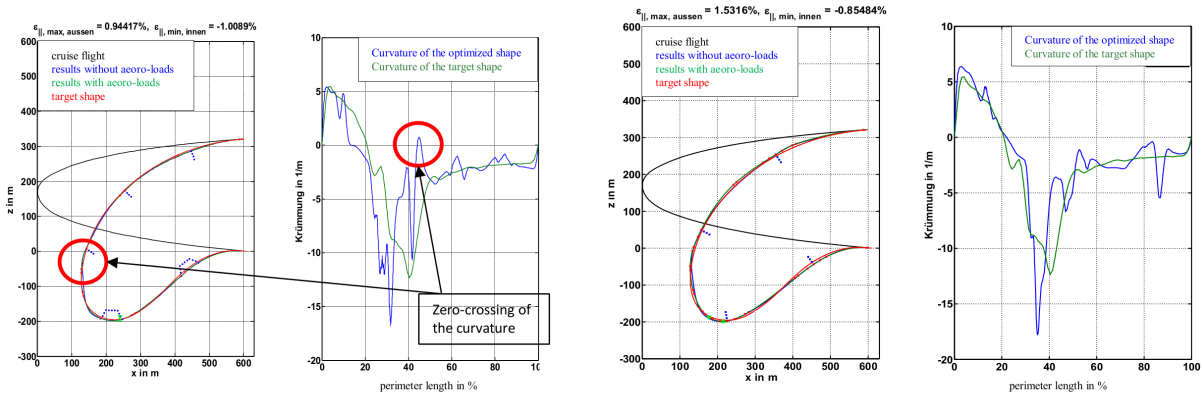

Figure 5. Results of the skin optimization for different force application concepts: 2xOmega- and 3xT- stringer (left), 4xT-stringer (right)

nodes deformations with respect to the actuator forces and has additionally an integrated procedure for determining the sensitivities of topology optimization design parameters presented in equation (5).

The objective function Z for the compliant kinematics is defined as a normed difference between the target position of the force application nodes U_{target} and the nonlinear finite element solution U which is calculated in the first optimization step:

$$Z = ||U_{\text{target}} - U|| = \left(U_{\text{target}} - U\right)^T \boldsymbol{T} \left(U_{\text{target}} - U\right) \tag{2}$$

The matrix $\boldsymbol{T}$ is used here to select the degrees of freedom that are to be used for the formulation of the objective function. These in particular are the degrees of freedom of the elements that contain the force introduction points from the first optimization step. Due to the fact that a SIMP approach prescribes a grid of equal (rectangular) elements, an additional interpolation of the force introduction points on the skin into the elements of the grid has to be performed. Therefore an interpolation matrix with Lagrangian polynomials is implemented according to equations (3) and (4) and also shown in Figure 6.

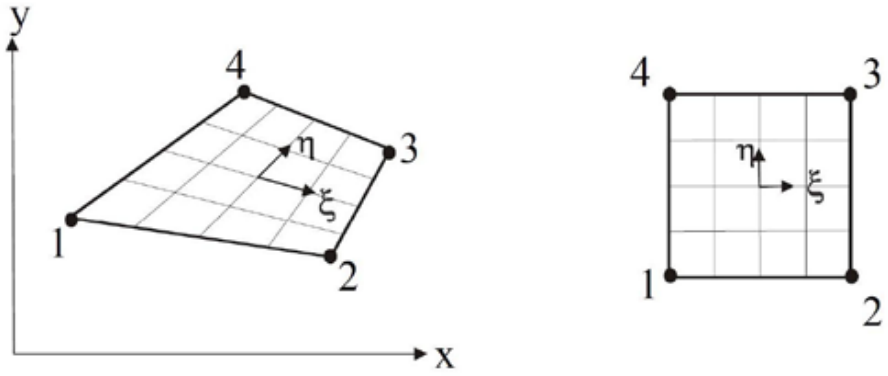

Figure 6. Cartesian and element coordinate systems in a deformed element

$$N_L = L_i^M(\xi) L_j^N(\eta) \tag{3}$$

$$U_i = N_L(\xi, \eta)\hat{x} \tag{4}$$

where U_i describes the position of the force introduction point inside of the element as a function of the preselected element nodes positions $\hat{x} = \boldsymbol{T}U$.

The sensitivities of the objective function Z with respect to the design variables x can be defined as

$$\frac{dZ}{dx} = -2\left[\dot{f} - \sum p\rho^{p-1} f_{\rho,el}(u)\right]^T \cdot \boldsymbol{K}_{TM}^{-1} \cdot \boldsymbol{T}\big(U_{\text{target}} - U\big). \tag{5}$$

Further definitions here are:

- $\boldsymbol{K}_{TM}^{-1}$ as an inverse tangential stiffness matrix of the finite element grid
- $\dot{f}$ as derivative of the actuator forces with respect to the design variables
- ρ as a pseudo density of a finite element
- a penalty factor p
- the non-linear stiffness of an element $f_{\rho,el}(u)$

The following finite element based approach has been developed in order to efficiently derive the matrices for the underlying static non-linear elasticity problem. The elastic constitutive equations consist of the usual linear equations for isotropic material under planar stress conditions

$$\begin{bmatrix}\sigma_x \\ \sigma_y \\ \tau_{xy}\end{bmatrix} = \rho^p \frac{D}{h} \begin{bmatrix}1 & \nu & \\ \nu & 1 & \\ & & (1-\nu)/2\end{bmatrix} \begin{bmatrix}\varepsilon_x \\ \varepsilon_y \\ \gamma_{xy}\end{bmatrix} \quad \text{with} \quad D = \frac{Eh}{1-\nu^2} \tag{6}$$

with the Young modulus E, the Poisson ratio ν, the membrane thickness h to couple the second Piola stress tensor σ with the Cauchy Green strain tensor ε in a geometrically non-linear way. Therefore we have

$$\varepsilon_x = u_{,x} + (u_{,x}u_{,x} + v_{,x}v_{,x})/2, \tag{7}$$

$$\varepsilon_y = v_{,y} + (u_{,y}u_{,y} + v_{,y}v_{,y})/2, \tag{8}$$

$$\gamma_{xy} = u_{,y} + v_{,x} + (u_{,x}u_{,y} + v_{,x}v_{,y}). \tag{9}$$

The virtual stiffness energy is then given by

$$\delta W_{\text{stiff}} = h \int_A \underbrace{\delta\varepsilon_x\sigma_x + \delta\varepsilon_y\sigma_y + \delta\gamma_{xy}\tau_{xy}}_{=\delta w_{\text{stiff}}} \, dA \approx h \sum_{e=1}^{m} \sum_{k=1}^{n_e} \left[\delta w_{\text{stiff}} \underbrace{\frac{\partial(x,y)}{\partial(\xi,\eta)}}_{=J} q_k^e \right]_{(\xi=\xi_k^e, \eta=\eta_k^e)} . \tag{10}$$

For the SIMP approach we use an elementwise constant density $\rho \in [0, 1]$ to establish a continuously varying stiffness between no material ($\rho = 0$) and full material ($\rho = 1$). A typical value for the penalty factor would be $p = 3$ in order to tag intermediate stiffness values with a penalty in the optimization process. The approximation in equation (10) uses numerical integration by suitable n_e Gauss points

with weights q_k^e in local coordinates (ξ_k^e, η_k^e) for each of the m elements. The usual finite element based approach would be to generate deformation dependent element stiffness matrices, which have to be assembled into the global stiffness matrix $\boldsymbol{K}_{TM}$. In a software environment like *MATLAB* with efficient vector based calculation routines it is hard to obtain an efficient solution for such assembly method. A careful observation of equation (10) after substitution of the constitutive equation (6) and subsequently the strains from (7–9) reveals, that the virtual stiffness energy δW_{stiff} consists of a sum of terms

$$D \sum_{e=1}^{m} \sum_{k=1}^{n_e} q_k^e f_{e,k}^{[1]} \cdot \dots \cdot f_{e,k}^{[r]} \tag{11}$$

where each $f^{[j]}$ is either a function δu, δv, u, v, x, y, ρ^p or a derivative of such a function with respect to ξ or η, evaluated at all Gauss integration points for each element. The whole assembly process can eventually be formulated by the combination of four basic tasks:

- The projection $\mathcal{P}$ of a field u, v, x, y, ρ or its derivative onto the Gauss integration points using the vector of elementwise constant densities $\boldsymbol{\rho}$ and the nodal deformations $\boldsymbol{u}$, $\boldsymbol{v}$.
- The multiplication $\mathcal{M}$ of vectors $\boldsymbol{f}^{[j]}$, which is an efficient pointwise operation.
- The assembly $\mathcal{A}$ of vectors on the Gauss points by a scheme suitable to respect the variations δu, δv or its derivatives. To obtain sensitivity information with respect to densities an assembly of $\delta\rho$ is also needed.
- The sparsity operator $\mathcal{S}$ for a pair of field types as explained in equation (12) to generate sparse system matrices.

$\mathcal{P}$ and $\mathcal{A}$ are adjunct rather than inverse operators. If for example $\boldsymbol{u}$, $\boldsymbol{v}$ are nodal values for the fields u, v and $\boldsymbol{f}$ is a vector of values on the Gauss integration points, we have

$$\big(\mathcal{P}_u\big[\boldsymbol{u}\big]\big)^T \boldsymbol{f} = \boldsymbol{u}^T \mathcal{A}_u\big[\boldsymbol{f}\big], \quad \big(\mathcal{P}_u\big[\boldsymbol{u}\big]\big)^T \operatorname{diag}\big(\boldsymbol{f}\big)\mathcal{P}_v\big[\boldsymbol{v}\big] = \boldsymbol{u}^T \mathcal{S}_{u,v}\big[\boldsymbol{f}\big]\boldsymbol{v}. \tag{12}$$

Because the interpolation of the fields is done on a regular nodal grid for the standard SIMP approach, these projection, assembly and sparsity operators can be implemented very efficiently. We have implemented these rather general operators in the programming language *C* as so called *MEX*-extensions to *MATLAB*. There are several field orders implemented. We currently only use the zero order for elementwise constant density fields and the first order bilinear interpolation for the deformation fields u and v. The implementation is also simultaneously done for one-dimensional, two-dimensional and three-dimensional domains. Again currently only the second case is used. The charme of this approach is its generality. The Ritz/Galerkin matrix equations of a huge class of partial differential equations can be coded based on these basic operations in a simple and efficient way. Even the memory consumption of this approach has the same order as classical finite element codes. And special needs as for example sensitivity information is also easily implementable. One limitation of this method is the use of a regular grid as basic mesh. This is no fundamental restriction as the operators have been successfully generalized in an efficient way for heterogeneous meshes. Another limitation is more severe. We only consider one element type in each single assembly process. Therefore different finite element types have to be assembled seperately. And the vector and matrix operations needed for more complicated elements like beam and shell elements must be expanded into scalar equations, which reduces efficiency and enhances coding complexity simultaneously. Luckily, for topology optimization all these restrictions are

usually not present, leading to a very efficient assembly procedure of the needed matrix equations for the elasticity equations.

An evaluation of the objective function and its derivatives is performed by the globally convergent version of the method of moving asymptotes (GCMMA). A detailed explanation of the method and its application in a topology optimization chain can be found in [9]. Depending on the defined convergence criteria (in this case a maximum allowable deviation from the target trajectories), the framework proceeds with updating the design parameter vector x or provides an optimized topology as a pre-design solution for further detailed design of the compliant kinematic. A preliminary result of the topology optimization is shown in Figure 7. In this case a compliant kinematic with one variable actuator force (red arrow) and one target displacement, representative for a force introduction point of the skin was optimized. It is clearly observable that the target position of the control point is reached by the mechanism with quite small deviation.

The implementation of a complete set of boundary conditions representative for a droop nose skin with appropriate constraints (number of force application points, advanced actuation system, installation space) will follow in the next future. For the latter more ambitious goals, the objective function and possibly also the optimization routine must be modified in order to achieve convergence, because the lack of convergence was observed for multi point targets of deflection shapes with highly non-linear deformations.

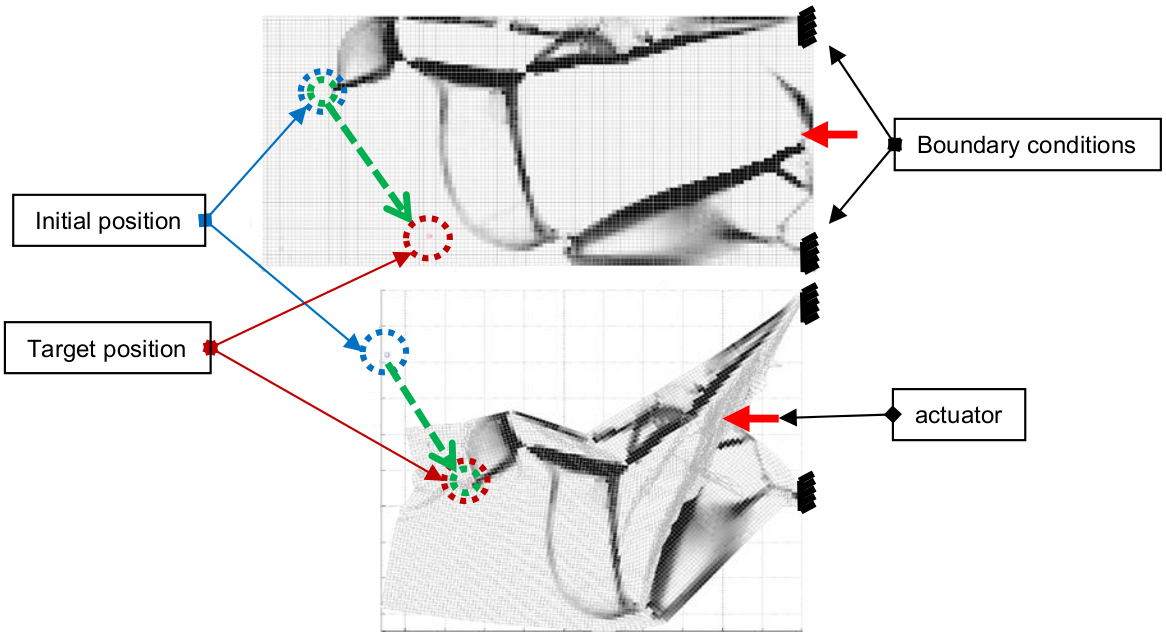

Figure 7. Preliminary results of the topology optimization

5. CONCLUDING REMARKS

A structural optimization framework is set up for an adaptive leading edge device with a high grade of

deflection. The maximal deviation from aerodynamic reasonable shapes for different flight (deflection) conditions provides the objective function for the optimization. Two different optimization methods are combined to obtain a morphing solution: a fast and robust simplex optimization of the skin stiffness distribution and a gradient based topology optimization of the non-linear deformed compliant kinematic system. The derivation of the compliant inner mechanism, which currently works for linear elasticity problems, but still has convergence problems for multi point highly non-linear problems must be enhanced regarding the objective function and/or the underlying optimizer, but the efficient underlying solution procedures for the elasticity subproblem have been proven to be mature. The neccessary post processing of the derived mechanisms is another ongoing work. The tool chain itself is already very promising and extensions to three-dimensional problems are also planned.

ACKNOWLEDGEMENTS

Financial support has been provided by the German Research Foundation (Deutsche Forschungsgemeinschaft — DFG) in the framework of the Sonderforschungsbereich 880.

REFERENCES

1. Barbarino, S., Bilgen, O., Ajaj, R. M. and Friswell, M. I., "A Review of Morphing Aircraft", *Journal of Intelligent Material Systems and Structures*, Vol. 22, 2011, pp. 823–899.
2. Sofla, A. Y. N., Meguid, S. A., Tan, K. T. and Yeo, W. K., "Shape morphing of aircraft wing: Status and challenges", *Material & Design - MATER DESIGN*, Vol. 31, 2010, pp. 1284–1292.
3. Kintscher, M., Wiedemann, M., Monner, H. P., Heintze, O. and Kühn, T., "Design of a smart leading edge device for low speed wind tunnel tests in the European project SADE", *International Journal of Structural integrity*, Vol. 2, No. 4, 2011, pp. 383–405.
4. Kintscher, M. and Wiedemann, M., *Design of a smart leading edge device. Adaptive, Tolerant and Efficient Composite Structures*, Springer Verlag, New York 2012, pp.381–390.
5. Burnazzi, M. and Radespiel, R., "Design of a Droopnose Configuration for a Coandă Active Flap Application", *51st AIAA Aerospace Sciences Meeting Grapevine*, Texas, January 2013.
6. Dodds, R. H. and Lopez, L.A., "Substructuring in Linear and Nonlinear Analysis", *International Journal for Numerical Methods in Engineering*, Vol. 15, 2013, pp. 583–597.
7. Hellen, T. K., "Use of substructuring in non-linear material analysis.", *Engineering Computations*, Vol. 1, No. 4, pp. 343–350.
8. Sigmund, O., "On the Design of Compliant Mechanisms Using Topology Optimization", *Mechanics of Structures and Machines: An International Journal*, Vol. 25, No. 4, 1997, pp. 493–524.
9. Bendsøe, M. and Sigmund, O., *Topology Optimization Theory, Methods and Applications*, Springer Verlag, New York, 2nd ed. 2003.
10. Saxena, A. and Ananthasuresh, G. K., "Topology Synthesis of Compliant Mechanisms for Nonlinear Force-Deflection and Curved Path Specifications", *Journal of Mechanical Design*, Vol. 123, 2001, pp. 33–42.